The Amide I Mode of Peptides in Aqueous Solution Involves Vibrational Coupling between the Peptide Group and Water Molecules of the Hydration Shell

Guido Sieler and Reinhard Schweitzer-Stenner*

Contribution from the FB1-Institut für Experimentelle Physik, Universität Bremen, 28359 Bremen, Germany

Received March 19, 1996[⊗]

Abstract: We have measured polarized Raman spectra of the model peptides glycylglycine and *N*-acetylglycine in aqueous solution with different excitation wavelengths. The spectra in the region between 1500 and 1800 cm^{-1} were consistently analyzed by using the same band shapes, halfwidths, and frequencies to fit the profiles of corresponding Raman bands. The quality and the statistical significance of the fits were judged by their residuals and reduced χ^2 numbers. This strategy enables us to obtain reliable spectral parameters of even strongly overlapping bands. Our experimental results show that the amide I bands of glycylglycine and *N*-acetylglycine in H_2O are composed of two subbands, whereas the corresponding amide I′ band of glycylglycine in D_2O can be fitted by one single band. Moreover, we found that the amide I band region in the Raman spectra of glycylglycine in different H_2O/D_2O mixtures (i.e., 25%/75%, 50%/50%, and 75%/25%) significantly deviate from the weighted superposition of the corresponding spectra of glycylglycine in pure H_2O and D_2O. These results are rationalized by invoking vibrational coupling between the amide I mode and the bending modes of the surrounding water molecules which provide a continuum of vibrational states. This coupling is absent in D_2O because deuteration causes a downshift of the water's bending mode. In H_2O/D_2O mixtures the undeuterated species exhibits a reduced splitting of its amide I band due to the lower density of H_2O molecules. Hence our results show that peptides and their aqueous environment form a dynamic entity. For glycylglycine the analysis of amide II also reveals a splitting into two subbands which most likely results from two different conformers with respect to the orientation of the carboxyl group.

Introduction

The amide I band in the IR and Raman spectra of polypeptides and proteins is widely used for the determination of these molecules' secondary structure. The structure sensitivity of this band results from the strong contribution of the CO stretch to its normal coordinate.[1,2] The force constant of the CO stretch is significantly altered by hydrogen bonding, involving the carbonyl group.[2,3] As a consequence, amide I of α-helices, β-sheets, random coil structures, and β-turns appear in distinct frequency ranges between 1630 and 1690 cm^{-1}.[2] Proteins composed of segments with different secondary structure thus gives rise to complicated broad and asymmetric amide I bands. Various computational strategies have been developed to decompose these bands into subbands assignable to well-defined secondary structures.[2,4]

An indepth understanding of the structure sensitive amide bands in the spectra of polypeptides requires knowledge of all interactions determining their normal mode composition.[2] To this end, significantly smaller molecules containing one or two peptide groups are frequently used as model systems for theoretical and experimental studies of the amide linkage in the above macromolecules. One of the classical model systems serving this purpose is *N*-methylacetamide ($CH_3CONHCH_3$, NMA). In an aqueous solution H_2O molecules form strong hydrogen bonds with the NH and carbonyl group of this molecule thus affecting the frequencies of all amide modes.[1,3,5] This in particular holds for the amide I vibration. By combining FT−IR, FT−Raman, polarized visible, and UV−Raman data, Chen et al. provided evidence that amide I is composed of two subbands at 1626 and 1646 cm^{-1}.[6] Normal coordinate calculations on a NMA−$(H_2O)_2$ complex suggests that this doublet arises from vibrational coupling of the NMA's amide I motion with the bending mode of water molecules hydrogen bonded to the peptide group. However, this theoretical calculation yielded a splitting of only 6 cm^{-1}, far less than the 20 cm^{-1} obtained from the experimental data. In order to rationalize this discrepancy, Chen et al.[6] proposed that amide I interacts with a range of HOH bending modes of water clusters constituting the peptide's aqueous environment. Most recently this model was further corroborated by *ab initio* calculations for NMA−$(H_2O)_2$ in a spherical cavity of radius 4.91 Å which is inserted into a medium of dielectric constant 20. The

* Author to whom all correspondence should be addressed (phone: **49-421-218-2509, Fax: **49-421-218-7318, E.Mail: stenner@theo.physik.uni-bremen.de).

[⊗] Abstract published in *Advance ACS Abstracts,* January 15, 1997.

(1) (a) Mirkin, N. G.; Krimm, S. *J. Mol. Struct.* **1991**, *242*, 143. (b) Mirkin, N.; Krimm, S. *J. Am. Chem. Soc.* **1991**, *113*, 9742. (c) Mirkin, N. G.; Krimm, S. *J. Mol. Struct.* **1996**, *377*, 219.

(2) (a) Krimm, S.; Bandekar, J. *Adv. Protein Chem.* **1986**, *38*, 181. (b) Bandekar, J. *Biochim. Biophys. Acta* **1992**, *1120*, 123.

(3) Wang, Y.; Purello, R.; Georgiu, S.; Spiro, T. G. *J. Am. Chem. Soc.* **1991**, *113*, 6368.

(4) (a) Williams, R. W. *J. Mol. Biol.* **19**??, *166*, 581. (b) Susi, H.; Byler, D. M. *Methods Enzymol.* **1986**, *130*, 290. (c) Surewicz, W. K.; Szabo, A. G.; Mantsch, H. H. *Eur. J. Biochem.* **1987**, *167*, 519. (d) Surewicz, W. K.; Mantsch, H. H. *Biochim. Biophys. Acta* **1988**, *952*, 115. (e) Dong, A.; Huang, P.; Caughey, W. S. *Biochemistry* **1990**, *29*, 3303.

(5) Gao, H.; Karplus, M. *J. Phys. Chem.* **1992**, *96*, 7273.

(6) (a) Chen, X. G.; Schweitzer-Stenner, R.; Mirkin, N. G.; Krimm, S.; Asher, S. *J. Am. Chem. Soc.* **1994**, *166*, 1141. (b) Chen, X. G.; Schweitzer-Stenner, R.; Asher, S. A.; Mirkin, N. G.; Krimm, S. *J. Phys. Chem.* **1995**, *99*, 3074.

S0002-7863(96)00889-X CCC: $14.00

calculation yields an amide I splitting of 23 cm^{-1} which is close to the value of 20 cm^{-1} observed for NMA.[6]

The Raman and IR band of the HOH bending mode appear rather broad ($\approx$110 cm^{-1}) which is indicative of a continuum of slightly different vibrational states. For aqueous NMA amide I nearly coincides with the maximum of the HOH band, thus enabling optimal vibrational mixing. Many secondary structures such as α-helices, random coils, and β-turns, however, exhibit their amide I band at higher frequencies, so that they merely overlap with the high frequency part of the HOH water band.[2] If the interaction model proposed by Chen et al.[6] applies, vibrational mixing should still occur in this case, but the amide I's splitting should be smaller than that observed for aqueous NMA. If this could be experimentally proven, the interaction between water and peptide motions would have to be regarded as relevant for the analysis of amide I modes of all peptides and proteins as well as for the physical understanding of protein−water interactions.[7]

These considerations prompted us to investigate the dipeptide glycylglycine (DGL: diglycin, $NH_3^+CH_2CONHCH_2COO^-$). Its amide I band is observed at 1688 cm^{-1}, thus overlapping only with the high frequency edge of the above water band and coinciding with the highest observed amide I frquencies of polypeptides. In this study, we have utilized polarized Raman spectra measured with different near-UV excitation to examine the composition of the spectrum between 1500 and 1800 cm^{-1}. To assess the possible influence of vibrational mixing between peptide and water motions, we extended the investigation to DGL in D_2O (DGLD, $ND_3^+CH_2CONDCH_2COO^-$) and H_2O/D_2O (DGLDH) mixtures. For comparison we also measured and examined polarized Raman spectra of the dipeptide *N*-acetylglycine (AGL, $CH_3CONHCH_2COO^-$) which exhibits its amide I band at 1636 cm^{-1}, very similar to NMA.

Materials and Methods

Material. Glycylglycine and *N*-acetylglycine were commercially obtained from Sigma Chemical Co. and dissolved in H_2O, D_2O, and different H_2O/D_2O mixtures without further purification. DGL concentrations ranged between 0.5 and 1.8 M. The AGL concentration was 1 M. For all experiments the solvent contained 0.25 M $NaClO_4$ whose 934-cm^{-1} Raman band was used as an internal standard.[8]

Experimental Setup. Most of the spectra were recorded by means of an excimer pumped dye laser with excitation wavelengths between 363- and 524-nm excitation. The pulse energy was 1 mJ at a 200-Hz repetition rate and a pulse length of about 10 ns. Thus an average laser power of 200 mW was provided. The incident beam was polarized perpendicular to the scattering plane, filtered by two pin holes, and focussed by a cylindrical lense of 40-cm focal length onto a spinning quartz cell. The measurements were carried out at room temperature. A polarization analyzer between the sample and the entrance slit enabled us to measure the intensity of the two components perpendicular and parallel to polarization of the exciting laser beam. A polarization scrambler was used to avoid different transmissions of the spectrometer for different polarizations. The scattered light was dispersered by a 500-nm blazed SPEX triple monochromator 1402 equipped with a 1200-grove/mm grating and detected by a CCD camera. This system provides 512 channels for data acquisition, thus covering a spectral range of 14.2 nm. The spectral window varies with the excitation wavelength on the wavenumber scale. It has a width of about 400 cm^{-1} for 400-nm excitation. Additionally we have measured spectra with a central grating position of 950 cm^{-1} in order to record the isolated ClO_4^- Raman line at 934 cm^{-1} which we have used as an internal standard for callibrating the intensities of the Raman lines. The collected data were stored in an IBM-AT computer for further analyses.

The spectral resolution is determined by the dispersion capability of the spectrometer, the distance between adjacent channels of the CCD camera, and the width of its entrance slit. It can be calculated by:[8b]

$$\Delta\Omega = \lambda^{-2}\frac{f\lambda/d + \Delta x_s^{\text{opt}}}{pf(\partial\theta/\partial\lambda)} \tag{1}$$

where $p = 20$ μm is the distance between adjacent channels, d and f are the diameter and the focal length of the concave mirror foccussing the dispersed light onto the spectrometer's exit slit, i.e., 12.5 cm and 60 cm, respectively, $\partial\theta/\partial\lambda$ denotes the dispersion of the spectrometer, Δ_s^{opt} is the spectrometer's slit width, and λ is the wavelength corresponding to the central grating position. Hence, assuming an entrance slit width of 50 μm, we obtain 4.3 cm^{-1} for $\lambda = 400$ nm.

Some spectra reported in this study were recorded with the CW excitation (406.7 nm) provided by a Kypton Laser (Coherent, Innova 90K). The measurements were again performed with backscattering geometry. By using a cylindrical lens of 10-cm focal length, the linear polarized beam was focussed onto the sample. The scattered light was collected and imaged on the entrance slit of the spectrometer, i.e., a Spex 1401 double monochromator equipped with 1200-grooves/mm grating, and detected by a CCD camera. Polarized Raman spectra were observed by using a polarization filter as analyzer placed in front of the entrance slit of the spectrometer followed by a scrambler. The entrance slit was adjusted to 100 μ. The corresponding slit width at the wavelength employed was 2.5 cm^{-1}.

Spectral Analysis. All spectra were transferred to a personal computer and subjected to a line shape analysis by the recently developed program MULTIFIT.[8b] This program allows appropriate base line corrections, deconvolution of highly overlapping bands by the Fourier self-deconvolution technique, and discrimination between Lorentzian, Gaussian and Voigtian band profiles. In order to obtain the true Raman band shapes, the observed bands were deconvoluted with the corresponding slit function of the spectrometer. The latter was determined by recording the spectral lines of several pencil lamps (e.g., neon, krypton, etc.) and can well be described by Gaussian functions. All spectra in this paper are shown normalized on the internal standard, i.e., the sodium perchlorate band at 934 cm^{-1}. To eliminate the broad depolarized H_2O Raman band at 1640 cm^{-1}, we have measured the solvent's reference spectra for both polarizations which were then subtracted from the corresponding peptide spectra by utilizing the Raman band of the internal standard. The IR spectra were treated in a similar way. The intensities of the Raman bands in the thus corrected spectra were derived from their band areas. The depolarization ratio (DPR) ρ was then calculated as:

$$\rho = I_\perp/I_\parallel \tag{2}$$

where $I_\perp$ and $I_\parallel$ denote the intensities measured with the polarizer oriented perpendicular and parallel to the incident polarization. From the polarized spectra we obtained the respective isotropic and anisotropic Raman scattering by:

$$I_{\text{aniso}} = I_\perp$$

$$I_{\text{iso}} = I_\parallel - \frac{4}{3}I_\perp \tag{3}$$

All isotropic and anisotropic Raman as well as IR spectra were consistently fitted in that the same band shapes, halfwidths, and frequencies of corresponding bands were used for corresponding data sets. The quality and the statistical significance of the fits were judged

(7) (a) Parak, F. *Methods Enzymol*. **1986**, *127*, 196. (b) Goldanskii, V. I.; Krupyanskii, Y. F. *Q. Rev. Biophys*. **1989**, *22*, 39. (c) Smith, P. E.; Pettitt, B. M. *J. Phys. Chem*. **1994**, *98*, 9700.

(8) (a) Current literature does not provide an unequivocal value for the frequency of this Raman band. In the present study we have used the emission lines of pencil lamps to determine its frquency with an accuracy of $\pm$0.5 cm^{-1}. (b) Unger, E.; Dreybrodt, W.; Schweitzer-Stenner, R. Manuscript in preparation.

(9) (a) Bevington, P. R. *Data Reduction and Error Analysis for the Physical Science*. MacGraw-Hill: New York, 1969. (b) Gilch, H.; Dreybrodt, W.; Schweitzer-Stenner, R. *Biophys. J*. **1995**, *69*, 214.

(10) (a) Song, S.; Asher, S. A. *J. Am. Chem. Soc*. **1989**, *111*, 4295. (b) Chen, X. G.; Li, P.; Holtz, J. S. W.; Chi, Z.; Pajcini, V.; Asher, S. A. *J. Am. Chem. Soc*. **1996**, *118*, 9705.

(11) Quian, W.; Krimm, S. *J. Phys. Chem*. **1994**, *98*, 9992.

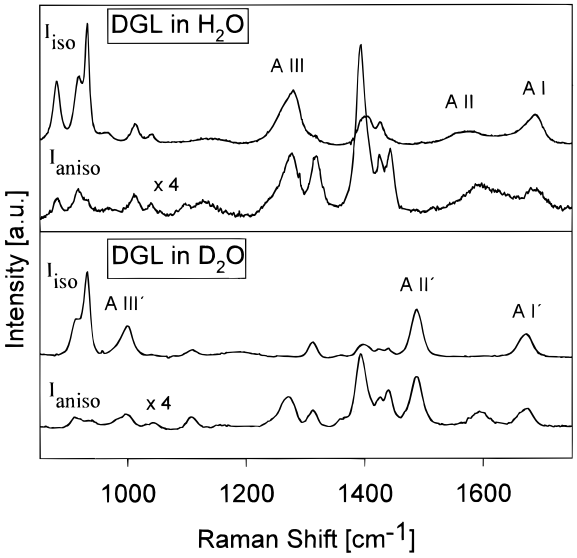

Figure 1. Isotropic and anisotropic Raman spectra of DGL (upper panel) and DGLD (lower panel) recorded between 800 and 1800 cm^{-1}. The spectra were obtained from polarized spectra measured with 406.7-nm (CW) excitation for DGL and 384-nm (pulsed) excitation for DGLD. The pH was adjusted to 6.8; the pD value to 6.2. Polarized reference spectra of the buffer were taken under the same conditions and subtracted from the originally measured Raman spectra. The most prominent Raman bands are indicated.

by their residuals and reduced χ^2 numbers. The latter is calculated by using:[9a]

$$\chi_R^2 = \sum_i \frac{(I_{i,exp} - I_{i,fit})^2}{\sigma_i^2 N} \quad (4)$$

where $I_{i,exp}$ and $I_{i,fit}$ are corresponding experimental and theoretically calculated intensities. σ_i denotes the statistical error of $I_{i,exp}$, which we determined from the noise of the measured spectrum. N is the number of data points in the spectrum. The number of free parameters was always small compared with N and is therefore neglected in eq 4. The sum runs over all data points. Acceptable and statistical significant fitting requires χ_R^2 values between 1 and 2.[9] $\chi_R^2 > 2$ means that the fit does not reproduce the data sufficiently well, while $\chi_R^2 < 1$ indicates that the fit is statistically insignificant. The above strategy enables us to obtain reliable spectral parameters of even strongly overlapping bands.

Results and Discussion

Glycylglycine. Figure 1 shows the isotropic and anisotropic Raman spectra of DGL and DGLD observed with 406.7- and 384-nm excitation, respectively. For DGL the well-known structure sensitive bands amides I, II, and III are observed at 1688, 1583, and 1279 cm^{-1}, respectively. Amides I′, II′, and III′ of DGLD appear at 1490, 1675, and 1000 cm^{-1}. These bands were already identified in the UV-resonance Raman spectra of DGL.[10] Other bands, in particular between 1300 and 1500 cm^{-1}, appear quite intense. A detailed analysis will be given in a forthcoming paper. In this study we confine ourselves on the spectral region between 1500 and 1800 cm^{-1}.

Figures 2 and 3 depict the isotropic and anisotropic Raman spectra of DGL (panels A and B) and DGLD recorded between 1500 and 1800 cm^{-1}. Amides I and II appear rather broad. The latter seems to exhibit a noncoincidence between its positions in the isotropic and anisotropic spectra. As we will show below, this is to a major extent caused by a totally depolarized band assignable to the COO^- as vibration (as: antisymmetric stretch).

In a *first step* we employed the simplest possible model to analyze the Raman spectra of DGL. It comprised two amide

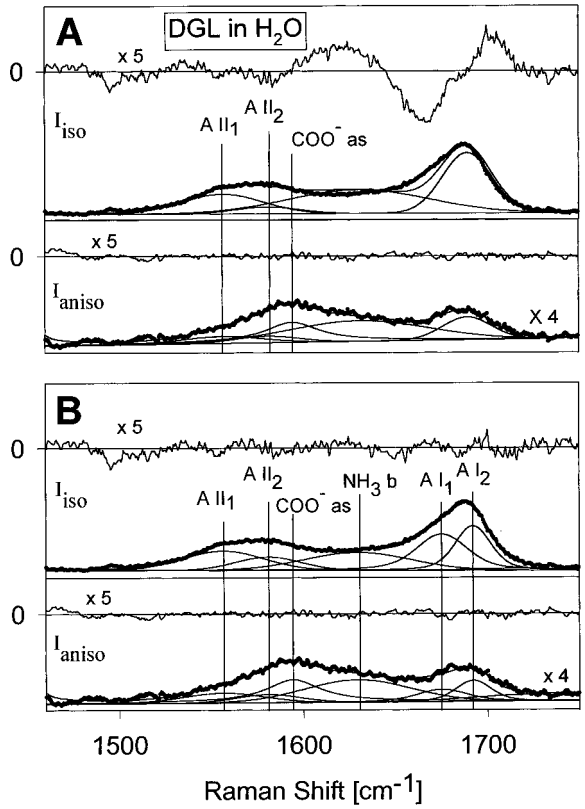

Figure 2. Spectral decomposition of the isotropic and anisotropic Raman spectra of DGL recorded between 1500 and 1800 cm^{-1}. The data were taken as described in legend of Figure 1. The dotted points represent the experimentally observed spectra. The single bands results from the band-shape analyses outlined in the text. The solid lines result from the fit to the data. Panel A exhibits the results obtained from a model assuming only one amide I band. Panel B depicts the fit based on a two-band model for amide I. The residuals of the fits displayed in the upper part of each panel are multiplied by a factor of 5 to facilitate the recognition of systematic deviations from pure noisy behavior.

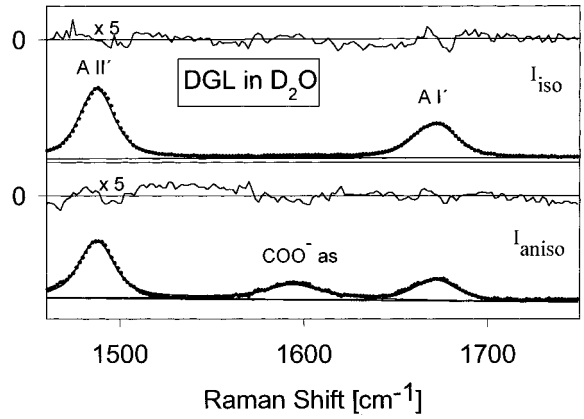

Figure 3. Spectral decomposition of the isotropic and anisotropic Raman spectra of DGLD recorded between 1500 and 1800 cm^{-1}. The data were taken as described in legend of Figure 1. The dotted points represent the experimentally observed spectra. The single bands results from the band-shape analyses outlined in the text. The solid lines result from the fit to the data. The residual of the fit displayed in the upper part of the figure is multiplied by a factor of 5 to facilitate the recognition of systematic deviations from pure noisy behavior.

(12) Schweitzer-Stenner, R.; Sieler, G.; Mirkin, N. G.; Krimm, S. *Proceedings of the XVth International Conference on Raman Spectroscopy*; Asher, S. A., Stein, P., Eds.; Wiley & Sons: Chichester, 1996; p 516.

Table 1. Spectral Parameters Derived from Fits to the Isotropic and Anisotropic Raman Spectra of DGL and DGLD Recorded between 1500 and 1800 cm^{-1}

mode	ν (cm^{-1})	Γ (cm^{-1}) Lorentzian	χ_R^2 Gaussian	χ_R^2 isotropic	χ_R^2 anisotropic
		(A) DGL in H_2O			
amide II_1	1556.6		51.9	1.54	1.07
amide II_2	1580.9		41.9		
COO^- as	1594.4	36.0			
NH_3	1629.5		68.25		
amide I_1	1675.3	14.6	23.6		
amide I_2	1692.2	7.7	18.0		
		(B) DGLD in D_2O			
COO^- as	1594.4	36.0			
amide I′	1671.3	13.1	20.4	1.91	1.85

II subbands (to account for the observed noncoincidence) and a single amide I band. This completely fails to reproduce the experimental data. The *second step* additionally comprises a depolarized band at 1595 cm^{-1}, which appears in the Raman spectra of DGLD and is therefore not assignable to amide II, and also a band between 1630 and 1640 cm^{-1}, the existence of which can be clearly inferred from the anisotropic spectrum of DGL (Figure 3). This yields the fit displayed by the solid lines in panel A of Figure 1. [Thereby we utilized the spectral parameters of the 1595-cm^{-1} band as obtained from the anisotropic spectrum of DGLD.] The fit is still inappropriate for the isotropic spectrum, as judged by the residuals and the χ_R^2 values of 3.53. Deviations between fits and experimental data are, in particular, significant for the low-frequency side of amide I, suggesting that it cannot be described by a single band. The *third step* therefore comprised two subbands of amide I. This indeed yields consistent and appropriate fits to the spectra as shown by the solid lines and residuals in Figure 2B. The χ_R^2 values fell well into the region indicative of reliable and statistically significant fitting. They are listed in Table 1, together with the spectral parameters and depolarization ratios obtained from the third fit.

We have further measured isotropic and anisotropic Raman spectra with different excitation wavelengths between 360 and 530 nm and found that all these spectra could well be fitted by the above spectral model, i.e., by using the same halfwidths, band shapes, and frequency positions. The isotropic part of three spectra taken with 363-, 436-, and 524-nm excitation are depicted in Figure 4 for illustration. The DGLD spectra are less complicated. They can consistently be fitted by a single Voigtian band for amide I′ and the above-mentioned depolarized band at 1594 cm^{-1}. The spectral parameters are also listed in Table 1.

The Raman bands identified in the spectra of DGL and DGLD can be assigned and characterized as follows. Amide II is composed of two polarized subbands, Sb_1(II) at 1556 and Sb_2(II) at 1580 cm^{-1}. Their DPR values are 0.16 ± 0.01 and 0.17 ± 0.05. [In a recent study, Chen et al.[10b] observed a somewhat larger DPR value of 0.22 for amide II with 488-nm excitation. One would obtain a similar value from the present data by neglecting the overlap with the depolarized band at 1594 cm^{-1}.] The depolarized band at 1594 cm^{-1} is not affected by deuteration and should be attributed to the antisymmetric stretch (COO^- as) of the carboxyl group.[11] The broad band at 1629 cm^{-1} which shows a DPR of 0.33 ± 0.03 most likely arises from the NH_3^+ bending mode.[11] Its disappearance in the spectra of DGLD results from the deuteration of the amino group. Finally the amide I band is found to be composed of two Voigtian subbands at 1674 (Sb_1(I)) and 1690 cm^{-1} (Sb_2(I)) with somewhat different DPRs, i.e., 0.09 ± 0.02 and 0.15 ± 0.02, respectively. In

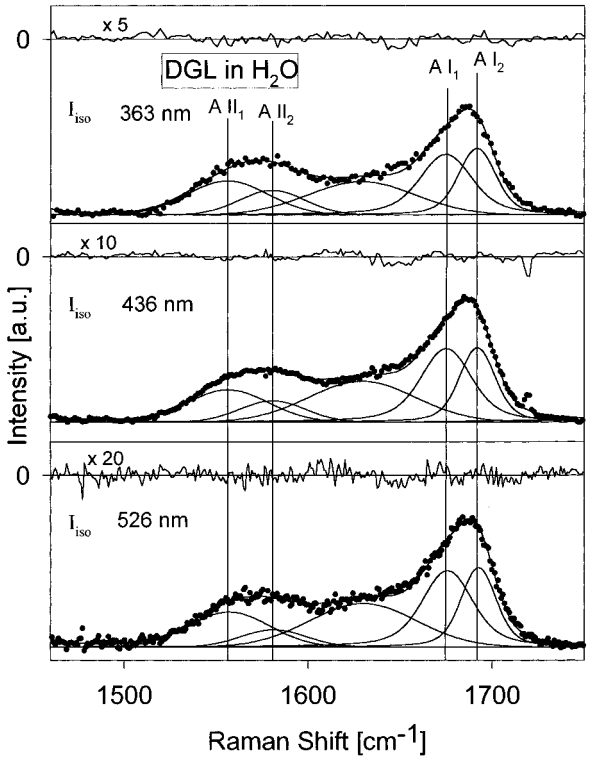

Figure 4. Spectral decomposition of the isotropic and anisotropic Raman spectra of DGL recorded between 1500 and 1800 cm^{-1} with 363-, 436-, and 536-nm excitation of an excimer pumped dye laser. Polarized reference spectra of the buffer were taken under the same conditions and subtracted from the originally measured Raman spectra. The dotted points represent the experimentally observed spectra. The single bands results from the band-shape analyses outlined in the text. The solid lines result from the fit to the data. The residuals of the fits displayed in the upper part of each panel are multiplied by the indicated factors to facilitate the recognition of systematic deviations from pure noisy behavior.

contrast, amide I′ comprises a single Voigtian band at 1671 cm^{-1} which exhibits a DPR of 0.14. Thus, all amide I and II bands are clearly polarized with depolarization ratios below 0.33, indicating that more than one electronic transition in the far-UV contributes to the scattering tensor.[6b,10b] This will be briefly discussed at the end of this paper.

One may argue that the amide I and II doublets in the spectra of DGL result from transition dipole coupling between corresponding modes of adjacent peptides which are aggregated by interpeptide hydrogen bonding.[1,11] This possibility, however, is not consistent with the absence of this splitting for the amide I′ band of DGLD. Moreover, we have measured the Raman spectra of samples with different DGL concentrations (i.e., 0.5, and 1.8 M) and found no differences (Figure 5). Taken together, this rules out that the two doublets result from the formation of DGL oligomers. We are, therefore, led to the conclusion that DGL parallels aqueous NMA in that its amide II mode reflects two different conformations, whereas the amide I doublet arises from vibrational mixing between amide I and the HOH bending modes of the aqueous environment.[1c,6b,c]

The appearance of structural heterogeneity is indeed not surprising. NMR experiments and molecular mechanics calculations on various dipeptides containing either as C-terminal or an N-terminal glycine revealed the existence of various rotamers with respect to the orientation of the peptide's COO^- and NH_3^+ group.[13] However, more experimental data combined with *ab initio* calculations are necessary to specifically assign

(13) Beeson, C.; Dix, T. A. *J. Chem. Soc., Perkin. Trans. 2* **1991**, 1913.

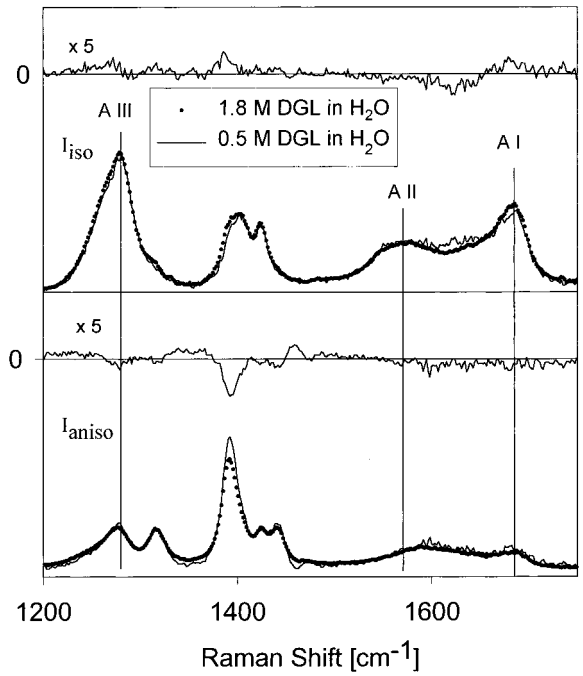

Figure 5. Isotropic (upper panel) and anisotropic (lower panel) Raman spectra of DGL between 1200 and 1800 cm^{-1} measured with 0.5 (solid line) and 1.8 M concentration (dotted points) at 384-nm excitation. The amide bands are indicated in the upper panel. The differences of these spectra are plotted in the upper part of each panel. The pH values were adjusted to 7.3 (0.5 M) and 7.5 (1.8 M).

the amide II subbands to distinct rotamers. In the following we therefore confine ourselves to the discussion of the amide I doublet.

If the amide I doublet indeed arises from vibrational mixing with water, amide I′ of DGLD should comprise a single band because the DOD bending mode appears at much lower frequencies. This is indeed observed (Figure 2B). Hence, one can also rule out the possibility that the amide I subbands result from peptides with different hydrogen bonding between their CO groups and adjacent water molecules. However, though conclusive, this finding does not provide a final proof of our assignment. One may argue instead that the subbands of amide I also reflect conformational heterogeneity while deuteration changes the normal mode composition to make this vibration's frequency less sensitive to conformational changes. Indeed, such an effect was recently obtained for amide II of NMA.[1c,6b]

To address this issue we employed the following protocol. First we measured polarized Raman specta of DGL dissolved in 25%/75%, 50%/50%, and 25%/75% H_2O/D_2O (volume) mixtures. These samples contain corresponding mixtures of DGL and DGLD. As shown in Figure 6 the spectrum of DGL dissolved in a 50%/50% mixture displays amides II and III as well as amides II′ and III′. We then determined the normalized intensities of these bands for all mixtures investigated and found them to depend linear on the mixing ratio (Figure 7). This shows that the solutes' concentration ratios correspond to the mixing ratios of the solvent. If amide I would indeed merely arise from conformational heterogeneity, one expects that the amide I* band (our notation for the amide I band in the spectra of H_2O/D_2O mixtures) of all isotopic mixtures can be reproduced by adding the correspondingly weighted spectra of pure DGL and DGLD. In the case of vibrational mixing with water, however, both amides I and I′ would change their band shape as a function of H_2O density.[14a] The splitting and also the

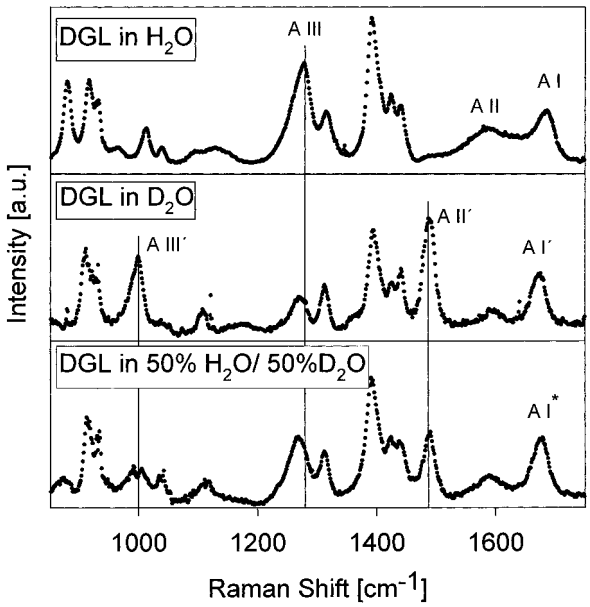

Figure 6. Unpolarized Raman spectra of DGL, DGLD in D_2O, and DGL in a 50% H_2O/50% D_2O mixture recorded between 800 an 1800 cm^{-1} with 443-nm excitation provided by an excimer pumped dye laser. The amide bands are indicated.

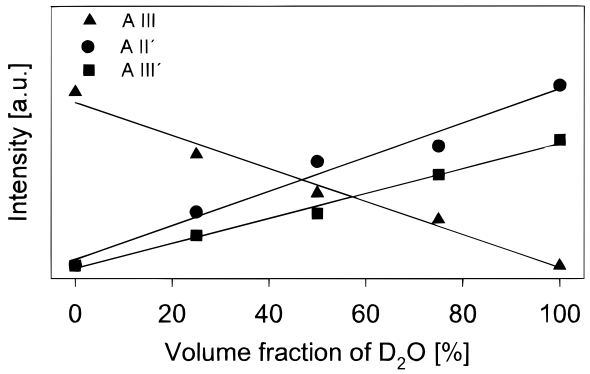

Figure 7. Raman intensities of amides I, II, and III as a function of the solvents' D_2O fraction as obtained from the spectral analysis procedure described under Material and Methods.

halfwidths[14b] of amide I would decrease when the above mixing ratio is reduced. Moreover, one expects some splitting of amide I′ which should increase with the mixing ratio. Thus, amide I* should be different from the weighted superposition of amide I and amide I′.

Figure 8 compares the amide I and II band region of the isotopic mixtures with the respective weighted superposition of the corresponding DGL and DGLD spectra. To facilitate comparison, the corresponding difference spectra are depicted on top of each panel. While the spectral bands of amide II, COO^- as, and NH_3^+ bending are always reproduced, amide I* appears significantly different from the superposition of amides I and I′ for H_2O/D_2O = 50%/50% and to a slightly minor extent for 75%/25%, while no significant difference is observed for 25%/75%. In the former cases, amide I* appears with a larger peak intensity, smaller width, and at slightly higher frequency than the corresponding superposition of amides I and I′. This observation clearly shows that the band shape of amide I depends on H_2O density and is therefore supportive of the notion

(14) (a) Hildebrandt, P.; Stockburger, M. *Biochemistry* **1984**, *23*, 5539. (b) Intermolecular vibrational mixing can be expected to facilitate energy transfer between the involved molecules, thus lowering the lifetime of the vibrational state and increasing the width of the Lorentzian part of the band profile.

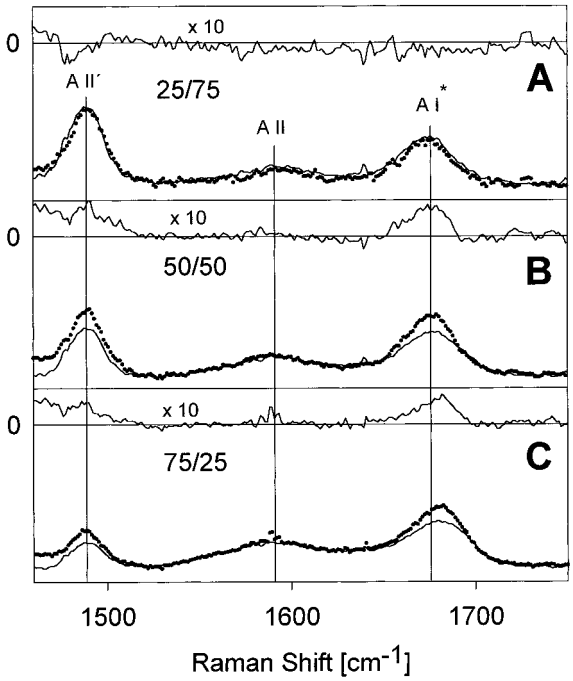

Figure 8. Comparison of the unpolarized Raman spectra (dotted points) of DGL in the indicated H_2O/D_2O mixtures with spectra generated as correspondingly weighted superposition of pure DGL and DGLD spectra (solid lines). The differences of these spectra plotted in the upper part of each panel are multiplied by a factor of 10 to facilitate the recognition of deviations from a pure noisy behavior.

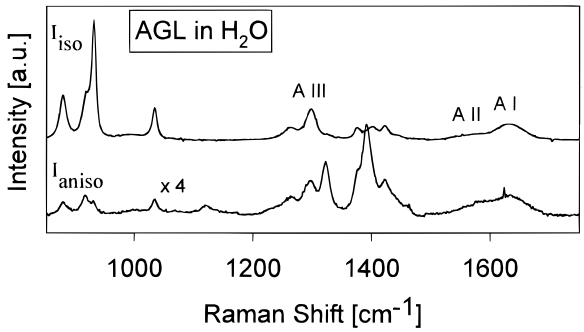

Figure 9. Isotropic and anisotropic Raman spectra of AGL recorded between 800 and 1800 cm^{-1}. The spectra were obtained from polarized spectra measured with 406.7-nm (CW) excitation for DGL. The pH was adjusted to 9.0. Polarized reference spectra of the buffer were taken under the same conditions and subtracted from the originally measured Raman spectra. The most prominent Raman bands are indicated.

that amide I is vibrationally mixed with bending vibrations of adjacent water molecules.

The spectra in panels B and C of Figure 8 show that the amide II′ region of the isotopic mixtures is also not reproducible by adding the spectra of DGL and DGLD. This can be explained if one takes into account that different subspecies of DGL and DGLD with NHD_2^+ and NH_2D^+ groups coexist. Thus, new bands may arise from their ND and ND_2 bending modes, which are expected to contribute to the spectral region between 1400 and 1500 cm^{-1}.[15]

***N*-Acetylglycine.** AGL is a dipeptide which is structurally inbetween NMA and DGL. Figure 9 exhibits its isotropic and anisotropic Raman spectra taken with 406-nm excitation. The positions of amides I, II, and III are similar to those observed for aqueous NMA. That in particular concerns amide I which has its peak frequency at 1634 cm^{-1}. Again we confine ourselves on the region between 1500 and 1800 cm^{-1}. The isotropic and anisotropic spectra for this region are shown in Figure 10. The spectral analysis was carried out by assuming that the band of the COO^- as appears with the same bandwith, frequency, and depolarization ratio as observed in the spectra of DGLD, whereas the band at 1629 cm^{-1} should be absent, because NH_3^+ is substituted by CH_3. A statistically reliable and significant fitting yields the result depicted in Figure 10. The spectral parameters are listed in Table 2. The amide I is composed of two still broad subbands at 1621 ($Sb(I_1)$) and 1644 cm^{-1} ($Sb(I_2)$). Thus they appear at slightly lower frequencies than those obtained for aqueous NMA[6b,c], whereas the splitting is identical in the limit of accuracy (i.e., 23 cm^{-1} for AGL and 20 cm^{-1} for NMA). This is what one would expect if this splitting really results from vibrational mixing between amide I and water. Amide II is rather broad, but in contrast to DGL the data do not allow an unambigious identification of subbands. However, differences between the amide II bands of DGL and AGL are expected because the latter lacks the electrostatic ion-pair interaction operative in the former dipeptide.[13] The DPR values are somewhat different from those obtained for DGL, i.e., 0.3, 0.2, and 0.21 for amide II, $Sb_1(I)$, and $Sb_2(I)$.

It should be mentioned that the χ_R^2 values of the above fits are somewhat lower than 1. This indicates that some parameters

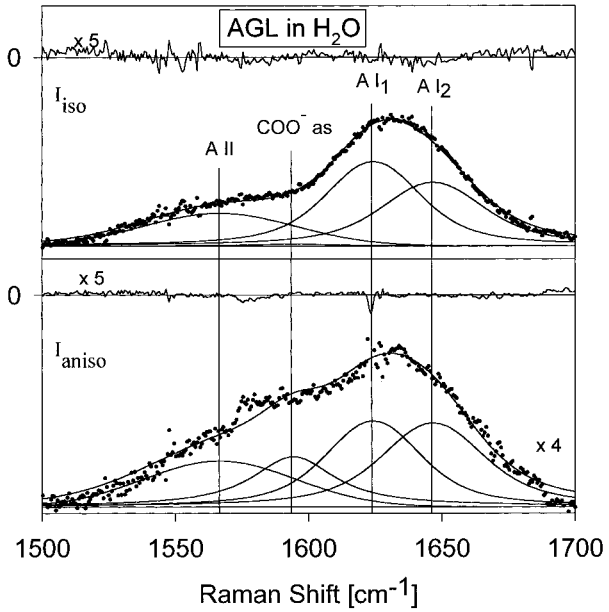

Figure 10. Spectral decomposition of the isotropic and anisotropic Raman spectra of AGL recorded between 1500 and 1800 cm^{-1}. The data were taken as described in the Materials and Methods section. The dotted points represent the experimentally observed spectra. The single bands results from the band-shape analyses outlined in the text. The solid lines result from the fit to the data. The residuals of the fits displayed in the upper part of each panel are multiplied by a factor of 5 to facilitate the recognition of systematic deviations from pure noisy behavior.

Table 2. Spectral Parameters Derived from Fits to the Isotropic and Anisotropic Raman Spectra of AGL Recorded between 1500 and 1800 cm^{-1}

		Γ (cm^{-1})	χ_R^2		
mode	ν (cm^{-1})	Lorentzian	Gaussian	isotropic	anisotropic
–	1544.4		31.1	0.88	0.74
amide II_2	1576.7		45.4		
COO^- as	1594.4	36.0			
amide I_1	1624.3	22.9	27.5		
amide I_2	1646.7	27.5	27.7		

(15) Faurskov Nielsen, O.; Mortensen, A.; Yarwood, J.; Shelley, V. *J. Mol. Struct.* **1996**, *378*, 1.

are not statistically reliable. This may in part result from uncertainties in determining the contribution of COO^- as. We like to emphasize, however, that any attempt to describe the data with a single amide I band yields inappropriate fits to both, isotropic and anisotropic scattering, as judged by the corresponding residuals and the χ_R^2 values.

Depolarization Ratios. For both dipeptides investigated in this study the DPR values of amide I and II are significantly smaller than 0.33 (with 406-nm excitation). This clearly suggests that their Raman cross sections gain contributions from Franck−Condon-type vibronic coupling to more than one electronic transition in the far-UV.[6a,b] The rather low DPR value obtained for $Sb_1(I)$ ($\rho = 0.09$) of DGL suggests that amide I is coupled to at least three transitions which cause the Raman tensor elements α_{xx}, α_{yy}, and α_{zz} to exhibit the same sign.[10b] That can be understood by recent findings which Chen et al.[10b] obtained from UV-resonance Raman and vacuum absorption spectra of DGL and related dipeptides. The authors identified a ca. 200-nm charge-transfer transition from the carboxylate nonbonding to the peptide's π^*-orbital and found that amides II and III are vibronically coupled to this transition. All amide modes, i.e., amides I, II and III, are also coupled to the peptide's 190-nm $\pi \rightarrow \pi^*$ transition. Additionally, amide I is significantly coupled to the second $\pi \rightarrow \pi^*$ transition of the peptide at even lower wavelengths.[10b,16] In the context of the present work it is noteworthy that the two amide I subbands of DGL exhibit somewhat different DPR values, i.e., 0.09 for $Sb_1(I)$ and 0.15 for $Sb_2(I)$. A similar observation has been made earlier for the two amide I subbands of aqueous NMA for which 0.14 and 0.22 was observed with 457- and also with 361-nm excitation. This was explained by assuming that the two amide I − H_2O modes are differently coupled to the peptide's $\pi \rightarrow \pi^*$ transition. This can also be expected to occur for DGL. The lower DPR values of DGL most likely result from additional contributions of the above charge transfer transition which is absent in NMA. We will discuss this issue in more detail in a forthcoming publication.

(16) Pajcini, V.; Chen, X. G.; Bormett, R. W.; Geib, S. J.; Li, P.; Asher, S. A. *J. Am. Chem. Soc.* **1996**, *118*, 9716.

Summary

Taken together, the results of the present study suggest that vibrational coupling between amide I and aqueous environment is a most general phenomenon and not limited to the special case of NMA. Hence evidence is provided that in accordance with most recent *ab initio* calculations for NMA−$(H_2O)_2$ the amide−HOH b interaction comprises a continuum of states which is reflected by the broad water band around 1640 cm^{-1}. Doubtlessly this has consequences for the interpretations of Raman and IR spectra of chemical and biological macromolecules which contain peptide groups. Moreover, it reveals that such systems and their aqueous environment constitute a dynamic entity. This may be of relevance for the understanding of vibrational dynamics and role of water for the function of biological molecules.

Acknowledgment. We thank Professor Samuel Krimm for providing us D_2O as well as him and Professor Sanford Asher for sending us copies of his papers prior to publication. Moreover, we are indepted to Professor Dreybrodt for his support of the project.

JA960889C